

An Experimental Investigation and Numerical Analysis on The Behavior Of Reinforced Concrete Thick Slabs under Static Loading

Adel A. Al-Azzawi¹

Ahmad S. Ali²

Yousif Kh. Yousif³

(Received 19/8/2016 ; accepted 16/10/2016)

ABSTRACT

This paper presents the testing results and numerical results of nine reinforced concrete thick slabs with and without openings. All slab specimens have the same planar dimensions ⁴(1000mm×1000mm) with three different thicknesses of (120mm,100mm,and 80mm).The slabs resting on 4 corner steel columns and tested under concentrated static loading up to failure. These slabs were also analyzed using nonlinear finite element method assuming nonlinear material properties. From the experiments, it was found that, The presence of openings in slabs supported on their four corners decreases the strength and rigidity of slabs to about (12-23) % depending on the slab thicknesses and the shape of these openings. The slabs with (circular opening) recorded a reduction in ultimate strength to about(20) % from those with square openings having an equivalent opening areas. The yielding of main steel reinforcement occurred at load about 85% of the slab ultimate load. The ultimate loads predicted by ANSYS model have showed a good agreement with the experimental results.

Keywords: Thick slab, Reinforced concrete, Slab with opening, Finite element, Nonlinear analysis.

التحري التجريبي مع التحليل العددي لسلوك السقوف الكونكريتية المسلحة السمكة تحت التحميل المستقر

أ.م.د. عادل عبد الأمير العزاوي أ.م.د. أحمد سلطان علي م.يوسف خلف يوسف

الخلاصة

يقدم هذا البحث نتائج الفحص المختبري والنتائج التحليلية لتسعة نماذج من السقوف الكونكريتية المسلحة السمكة الحاوية على فتحات وبدونها. جميع النماذج لها نفس الأبعاد (1000x1000) ملم بثلاثة سماكات (120، 80، 100) ملم. تم اسناد نموذج السقف اسنادا بسيطا باستخدام الواح فولاذية (125x125) ملم في كل من زوايا الأربع ، وتم اجراء الفحص تحت التحميل المركز الساكن لحين حدوث الفشل. كذلك تم اجراء تحليلات عددية- ثلاثية الأبعاد- لهذه النماذج باستخدام طريقة العناصر المحددة مع افتراض خصائص لا خطية للمواد. تبين من خلال الفحوصات المختبرية ان وجود الفتحات في السقوف المستندة- اسنادا بسيطا- في اركانها يؤدي الى انخفاض مقاومة السقوف بنسبة (12- 23) % اعتمادا على سمك السقف وشكل الفتحات. كما تم الاستنتاج بان السقوف ذات الفتحات الدائرية سجلت انخفاضا في الاحمال القصوى بنسبة (20) % عن تلك السقوف ذات الفتحات المربعة المكافئة بالمساحة لفتحات الدائرية. ، كذلك وجد ان السقوف لها استطالة فائقة عند الفشل. لقد اثبت نموذج التحليل العددي باستخدام برنامج (ANSYS) قدرته على التنبؤ بالأحمال القصوى ، حيث اظهرت النتائج توافقا جيدا مع الاحمال التجريبية.

1. Introduction

Reinforced concrete slabs are among the most well known types of structural members. In design of slab without beams, punching shear is one of the most critical problems, the use of slabs with large thicknesses was one of the successful solutions. This led to an experimental and

¹ Assist. Prof.at the Department of Civil Eng., Al- Nahrain University

² Assist. Prof. at the Department of Civil Eng., Baghdad University

³ Lecturer, at the Department of Civil Eng., University of Anbar.

analytical investigation to study the behavior of RC slab with different thicknesses under static loading. In this study, the geometry of all slabs satisfied the criteria $L/h \leq 10$ to be classified as thick or thin slab according to the Mindlin-Reissner theory[1]. This investigation includes studying the response of reinforced concrete thick slab (with and without openings) with different thicknesses under static loading. Due to lack of accurate calculation method, the magnitude of allowable load and the size of an opening are limited by building codes, therefore, knowing the distribution of stress in such structural members will form the backdrop to find new ways for reinforcing and making the design more flexible[2]. The study discusses the flexural behavior, deformation capacity, and cracking patterns. A three dimensional nonlinear finite element analysis has been carried out to investigate the ability of finite element method to predict the response of reinforced concrete thick slabs(with and without opening) under static loading.

2. Experimental Work

2.1 Details of thick slabs

The experimental program consists of nine slab specimens. They were divided into three groups according to shape of openings. All slabs specimens had identical planar dimensions(1000mm×1000mm) with three different thicknesses of (120mm, 100mm, 80mm) for each group. The first group consisted of three slab specimens without opening, the second group consisted of three slab specimens with square opening of (130×130)mm, while the third group consisted of three slab specimens with circular opening of (150mm in diameter). All openings have the same location at the center point of one half of the slab. The geometry and parameters for each specimen is summarized in Table (1). The main reinforcement consisted of (5 ϕ 8mm) steel bars in two directions. Dimensions and reinforcement of each slab are shown in Figure 1. The slab was simply supported by stiff steel plate at each corner.

Table (1): Geometry and Parametric Study of Experimental Work.

Group No.	Slab designation	Slab thickness mm	Opening shape	Opening size mm
1	SS 12	120	Solid	Solid
	SS 10	100		
	SS 8	80		
2	Sh13-12	120	Square	130×130
	Sh13-10	100		
	Sh13-8	80		
3	Shc15-12	120	Circle	150-daim.
	Shc15-10	100		
	Shc15-8	80		

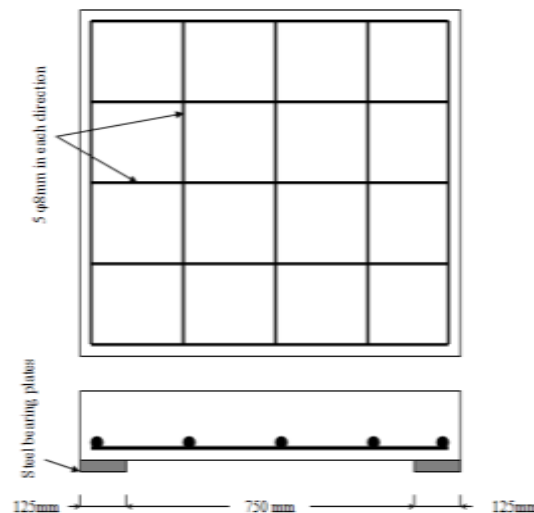


Figure (1): Dimensions and Reinforcement Details of Slab Specimens.

2.2 Material properties

All material tests were carried out by the researcher at the laboratory of Civil Engineering Department /Al- Nahrain University. The compressive strength test of concrete (f'_c) was made in accordance with ASTM C39/C39M-05[3]. 100×200mm cylindrical specimens were used to estimate the compressive strength of hardened concrete. Splitting tensile strength has been determined by testing three standard cylinders of (100×200mm) according to ASTM C496-04[4] specification. The flexural test was conducted using (100 x 100 x 400mm) prism specimens in conformity with ASTM C78-02[5]. The prisms were subjected to two- points load. Measurements of the static(secant) modulus of elasticity of concrete were made according to ASTM C469-02[6], using (150×300mm) concrete cylindrical specimens tested in compression. Mechanical properties of the hardened concrete and rebars for all thick slabs are summarized in Table (2) and Table (3).

Table (2): Test Results for Mechanical Properties of Hardened Concrete Specimens.

Group No.	Cylinder compressive strength f'_c (MPa)	Splitting tensile strength f_{ct} (MPa)	Modulus of Rupture f_r (MPa)	Modulus of elasticity E_c (MPa)
1	27.53	2.606	3.062	20590
2	28	2.701	3.238	20370
3	27.25	2.339	2.872	21070

Table (3): Mechanical Properties of Steel Bars Reinforcement.

Bar Nominal diameter (mm)	Bar Measured diameter (mm)	Yield Strength (MPa)	ultimate Strength (MPa)	Elongation %	Modulus of elasticity (GPa)
8	7.836	566.5	643.64	12.845	198.3

Note: tested steel bars reinforcement conformed to the requirements of grade 60 (60ksi), min. $f_y = 420$ MPa, min. elongation = 9% according to ASTM A 615-05 [7] for bars dia. 8mm

2.3 Testing Procedure

The slabs were simply supported at each corner using stiff steel plates of size 125x125 mm. All surfaces of the slabs were white painted to facilitate detection of concrete cracking. The loads were applied at increments rate of 0.5 kN/sec. The center midspan deflection of the slabs at each increment of load were stored in the computer software and then were used to graph and analyze the test results. First cracking loads (P_{cr}) and corresponding displacement at mid span (Δ_{cr}) were marked. When the slabs reached the failure stage the values of ultimate loads(P_{ult}) and ultimate displacement (Δ_{ult}) were recorded. Plate 1 show slabs setup on hydraulic testing machine.



Plate (1): Slabs Setup on Hydraulic Testing Machine.

3. TEST RESULTS

3.1 Concrete cracking and deformation

Table (4) summarizes the experimental results such as cracking loads, ultimate loads, deflections at first crack and deflection at failure for the slab specimens. For group 1, It is observed that, under loading, the first cracks (flexural) occurred at loads equal to (59,57 and 46)% of the ultimate loads for slab specimens (SS12, SS10, and SS8) respectively. Figure 2 show graphically the cracking and ultimate loads for the slab specimens. From this figure, with increasing the slab depth the cracking and the ultimate loads are increased.

For group 2, it can be seen that the first cracking loads of specimens (Sh13-12, Sh13-10, and Sh13-8) were the same values of solid specimens while the ultimate loads decreased by (14, 17, and 12)% from solid ones, respectively. For group 3, it can be observed that, the first cracking loads of specimens (Shc15-12, Shc15-10, and Shc15-8) show drop of first cracking load by (22, 21, and 12)% from solid specimens, respectively. Also, the specimens show drop of ultimate load at about (16, 23 and 17)% from solid specimens, respectively.

Table (4): First Cracking and Ultimate Loads for Thick Slab Specimens

Group No.	Slab designation	First crack load (kN)	Cracking midspan Deflection Δ_{cr} (mm)	Ultimate load (kN)	Deflection At Ultimate Load $\Delta_{Ultimate}$ (mm)	Mode of Failure
1	SS-12	44.1	3.41	74.29	21	Flexural
	SS-10	34.3	5.06	60.03	25	Flexural
	SS-8	19.6	2.19	42.26	19	Flexural
2	Sh13-12	44.10	3.12	63.50	24	Flexural
	Sh13-10	34.30	5.07	49.83	24	Flexural
	Sh13-8	19.60	3.36	37.13	17	Flexural
3	Shc15-12	34.3	2.38	62.26	19	Flexural
	Shc15-10	26.95	3.20	46.50	26	Flexural
	Shc15-8	17.15	2.87	34.93	22	Flexural

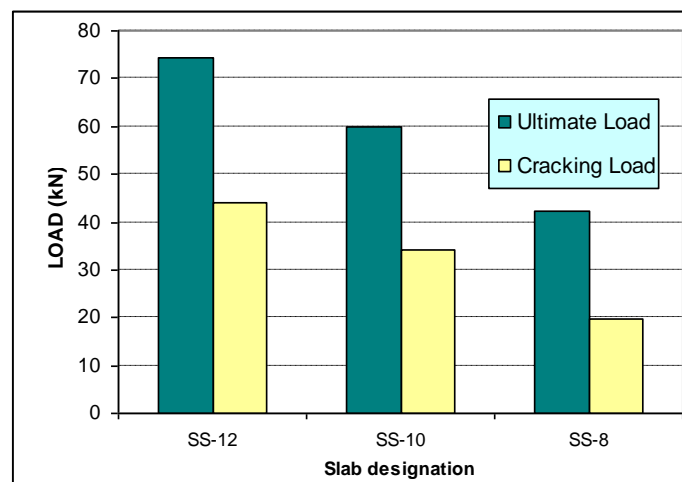
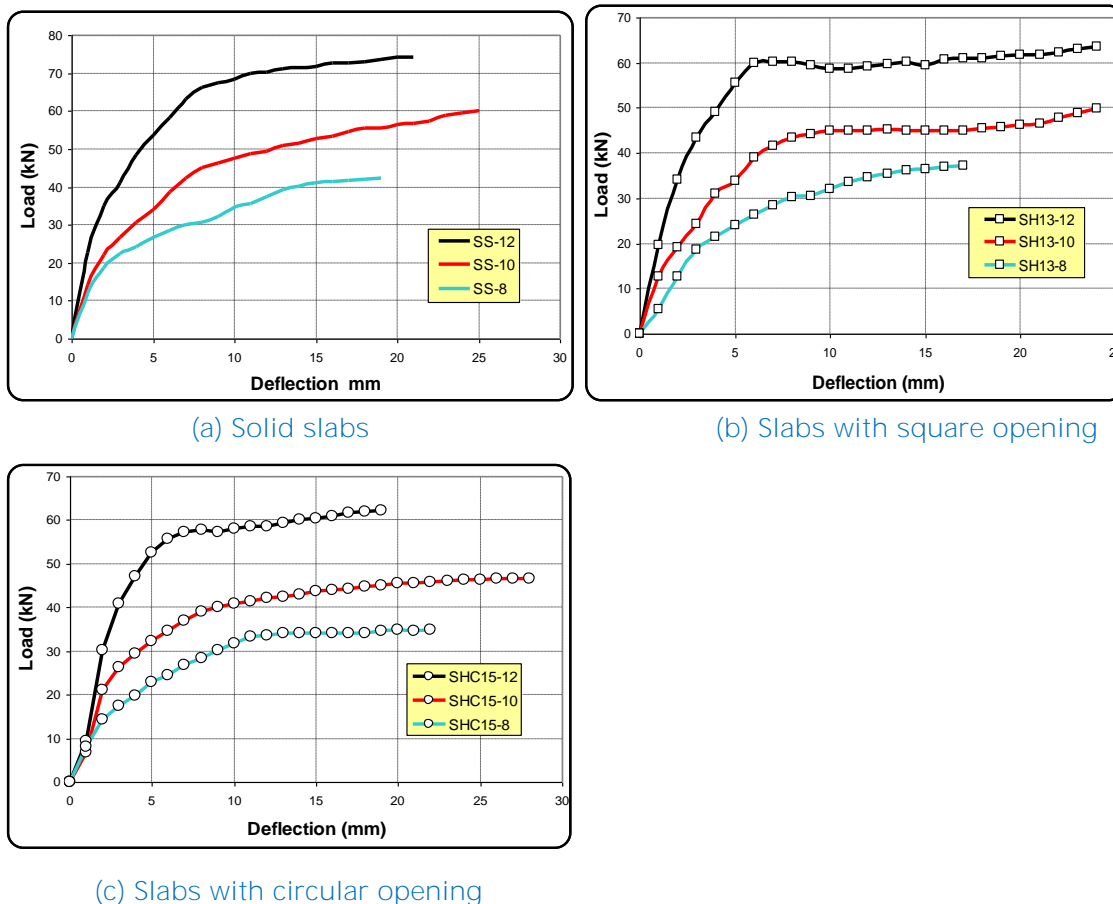


Figure (2): Effects of Slab Thickness on The Cracking and Failure Loads of Slab Specimens (SS-12), (SS-10) and (SS-8).

3.2 Load-deflection curves

Figure 3 illustrates the load-deflection curves for all slab specimens at the central point. The trend of deflection curves for all slabs was characterized by noticeable nonlinear behavior. Such a trend may be idealized by tri-linear diagram bounded by cracking point, yielding steel point and failure point. According to these load-displacement curves, the slabs had high deflection at the failure and the mode of failure can be considered as a ductile failure. The presence of openings in slab

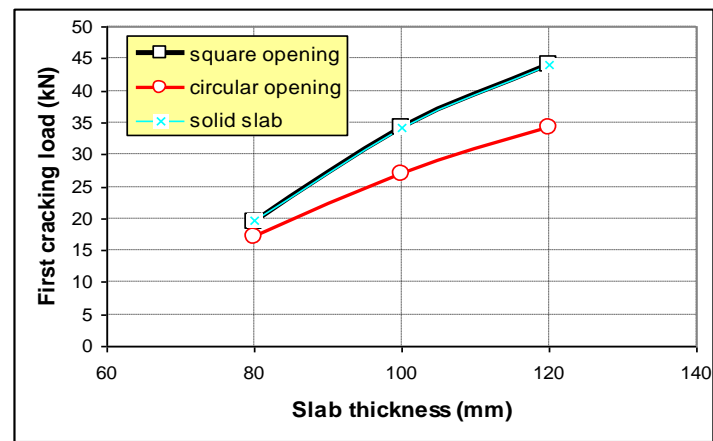
specimen decreases the ultimate loads by (12-23) % depending on the slab thickness and shape of these openings. The slab specimen SS-12 which had the maximum slab thickness (in this study) of 120mm, resulted in the maximum failure load of 74.29 kN with midspan deflection value of 21mm at failure. Also, it was observed that the slab specimen SHC15-8 which had slab thickness of 80mm and opening of 150mm diameter resulted in less failure load value of 34.93 kN with midspan deflection value of 22 mm at failure stage.



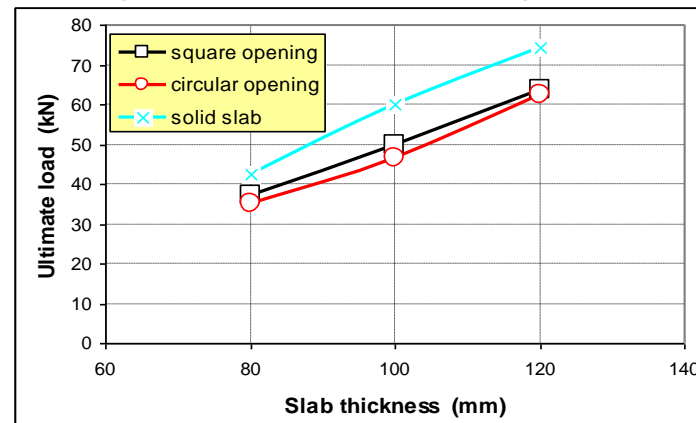
Figure(3): Load- Deflection Curves for The Tested Slab Specimens.

3.3 Effects of opening shape on slab behavior

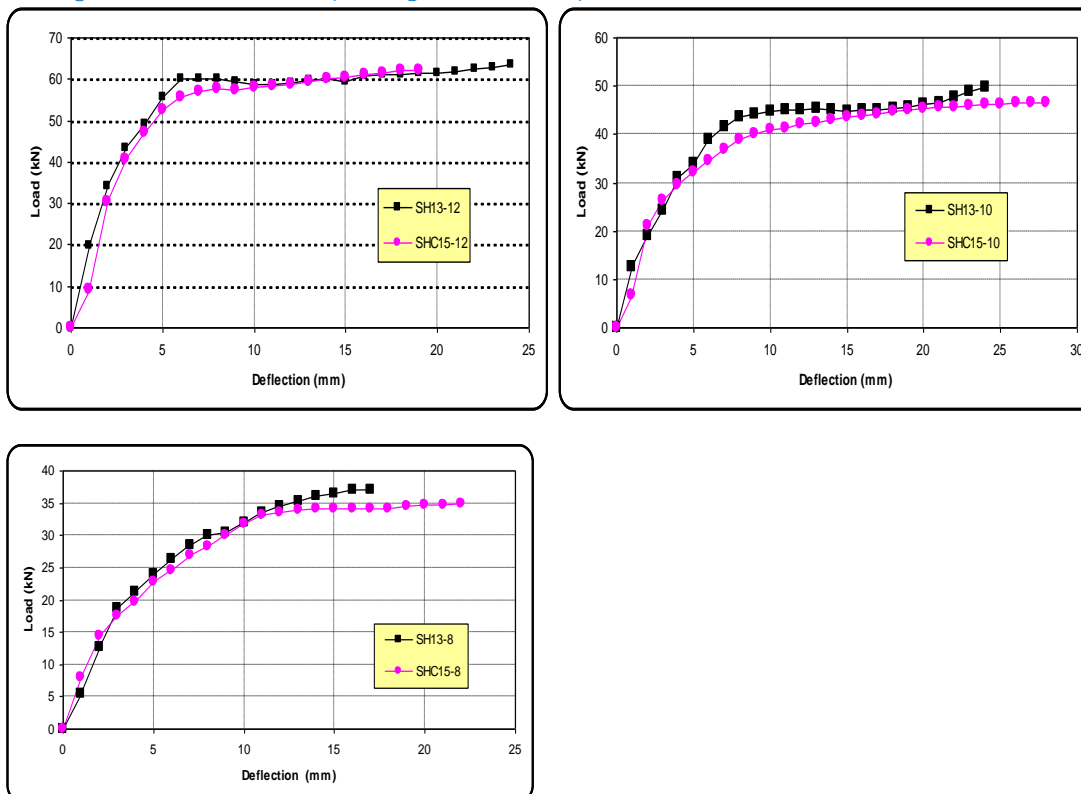
A comparative study has been conducted on slab specimens which have circular openings of 150mm diam. to be compared with the others which have an equivalent area of square opening of (130x130) mm. The effects of opening shape on cracking and ultimate loads of the tested specimens is shown in Figure 4 and Figure 5. From Figure 4, it can be seen that, all specimens with circular opening have smaller cracking loads compared with specimens of square opening. Also, all specimens with square opening have the same cracking loads of solid specimens. From Figure 5, it can be noted that, all specimens with circular opening have relatively lower ultimate loads compared with specimens of square opening, this might be because specimens with circular opening have larger ratio of (opening dimension to span length) compared with specimens of square opening. Load- deflection curves for all slab specimens which have circular openings were compared with that having square openings as shown in Figure 6.



Figure(4): Effects of Opening and its Shape on the Cracking Loads of Tested Slab Specimens



Figure(5): Effects of Opening and its Shape on the Ultimate Loads of Tested Slab Specimens

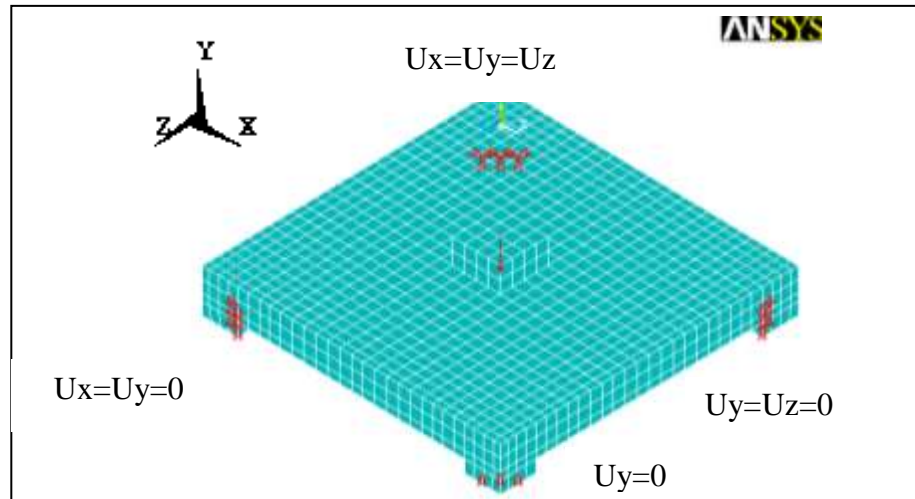


Figure(6): Comparison of Load- Deflection Curves for Slab Specimens with Circular Openings and Slab Specimens with Square Openings.

4. NUMERICAL RESULTS

4.1 Material representation

The slab was analyzed by nonlinear finite element method using ANSYS11.0[8] program. Various elements of ANSYS 11.0 were used to model the slab system. Solid65 and Link8 elements were used to model concrete and main reinforcement, respectively. Solid185 element was used to model the steel bearing plates. In this analysis, the reinforcement of the slab was modeled discretely by assuming that perfect bonding occurs between the concrete and the reinforcement. Finite element meshing and boundary conditions for slab specimens are shown in Figure 7.



Figure(7): Finite Element Meshing and Boundary Conditions for Thick Slab Specimens

4.2 Model Parameters

The finite element models used in this investigation have a number of parameters, which can be classified into the following:

- Concrete property parameters, Table (5).
- Steel bar property parameters, Table (6).
- Steel plates property, Table (7).

Table 5: Properties of Concrete

Parameter	Definition	Group 1	Group 2	Group 3
F'_c (MPa)*	Compressive strength	27.53	28	27.25
f_t (MPa)*	tensile strength	2.606	2.701	2.339
T_c^{**}	Tension stiffening parameter	0.6	0.6	0.6
B_0^{**}	Shear transfer parameters	0.3	0.3	0.3
β_c^{**}		0.8	0.8	0.8
E_c (MPa)*	Young's modulus of elasticity	20590	20370	21070
ν^{**}	Poisson's ratio	0.2	0.2	0.2

* Section 2.2

** Assumed value

Table 6: Properties of Steel Reinforcement

Parameter	Value
Bar diameter (mm)	7.836*
A_b (mm ²)	48.227
f_y (MPa)	566*
E_s (GPa)	198*
ν	0.3**
Tang Mod (MPa)	10000**

* Section 2.2

** Assumed value

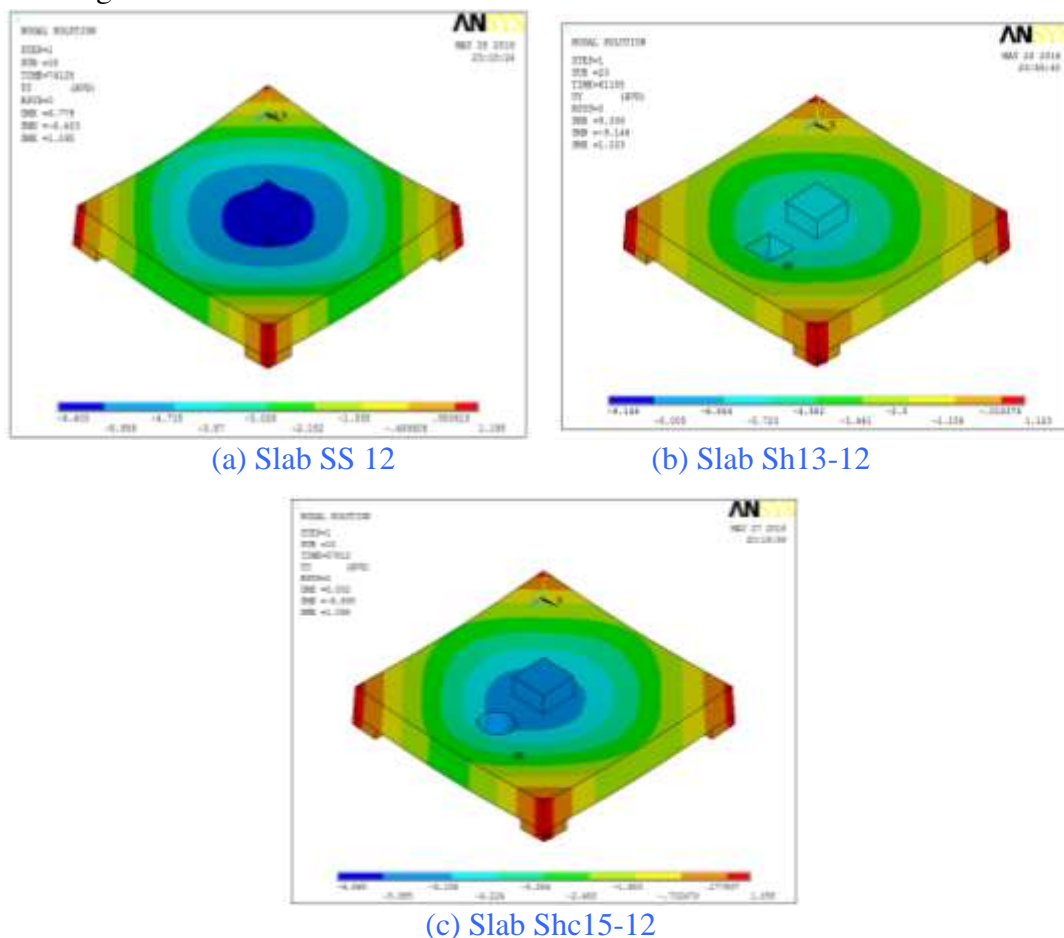
Table 7: Properties of Steel Plates

Parameter	Value
Thickness of steel plates	40 mm
Modulus of elasticity (E_s)	200*GPa
Poisson's ratio (ν)	0.3*
Material behavior	Linear elastic

* Assumed value

4.3 Load-Deflection Relation

Deflections were measured at the center of the bottom face of tested slabs. Deflected contours of finite element for thick slab (SS 12, Sh 13-12, and Shc 15-12) due to vertical concentrated load are shown in Figure 8.



Figure(8) : Deflection Contours of Thick Slabs (in mm)

5. NUMERICAL AND EXPERIMENTAL RESULTS

The numerical load-deflection curves and the experimental results are shown and compared in Figure 9. In general, these results show that the experimental results and the numerical results were in good agreement in the initial loading up to the yielding load. After yielding, the numerical results show different performances with the experimental results, this due to the difficulty of actual idealization of supports and material properties at plastic stage. It can be noticed from the load-deflection curves that the experimental results present higher deflection after yielding stage than the numerical results. However, the obtained loads from the analysis show close values with experimental results at the ultimate stage.

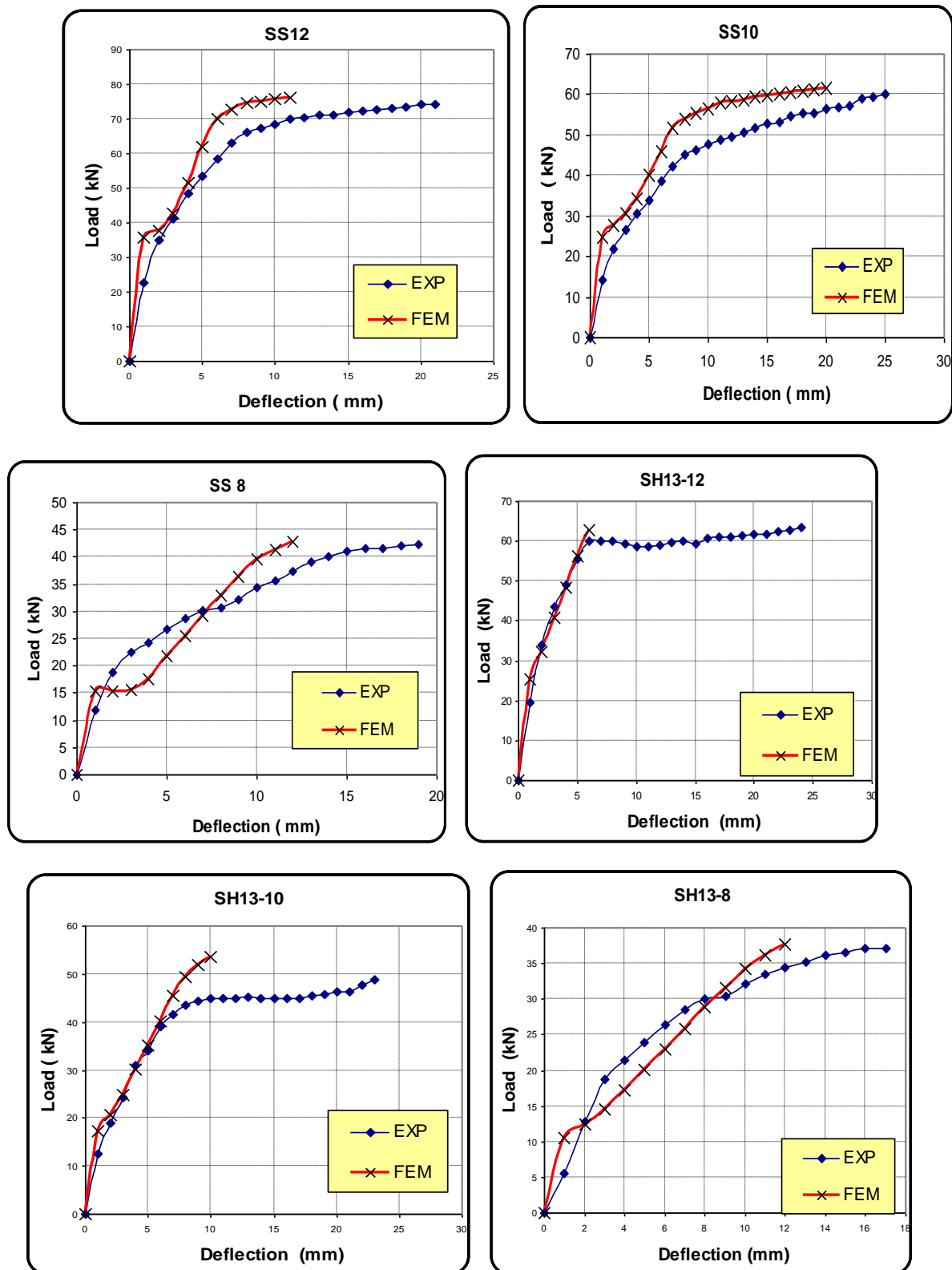
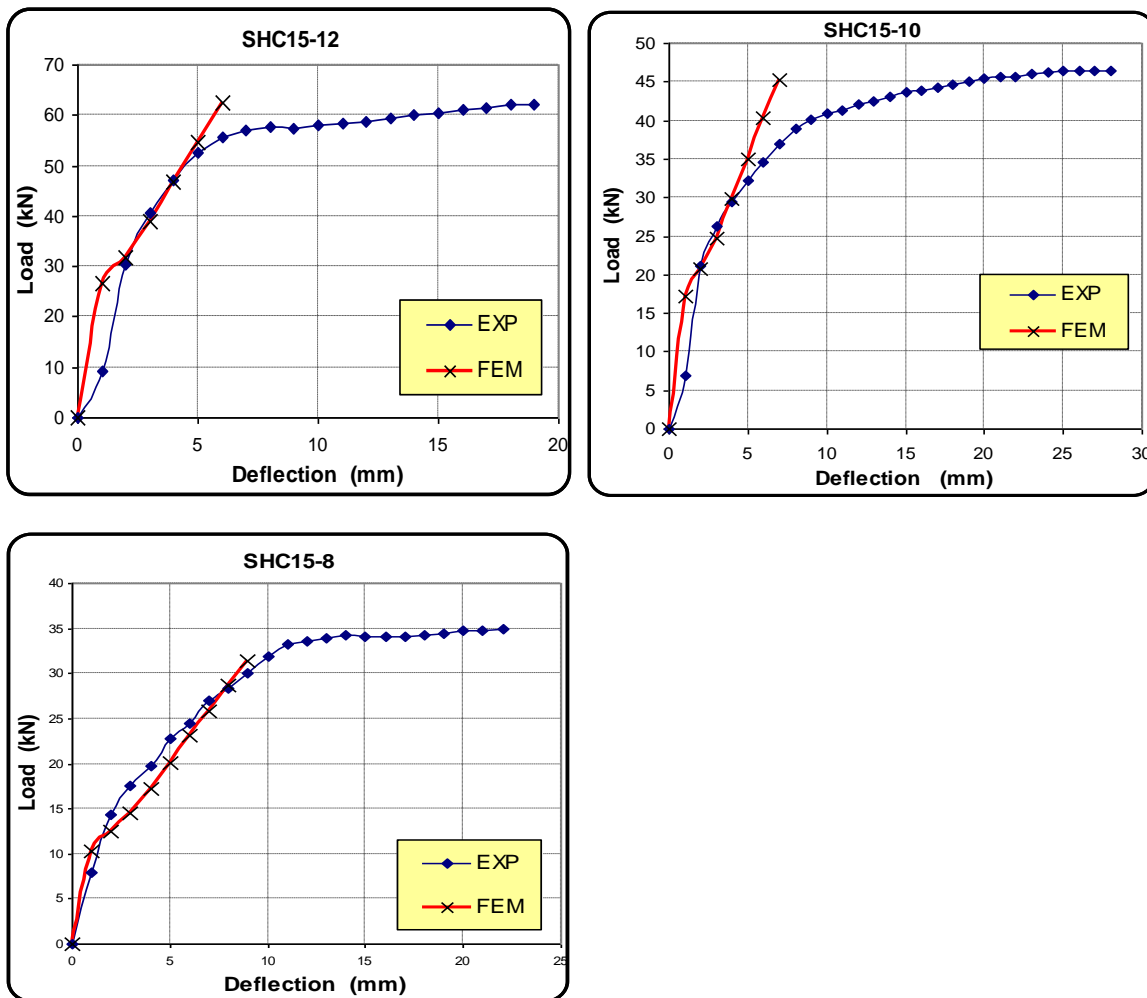


Figure (9): Load-Deflection Curves for Tested Thick Slab



Figure(9): Continued Load-Deflection Curves for Tested Thick Slab

5.1 Ultimate Loads

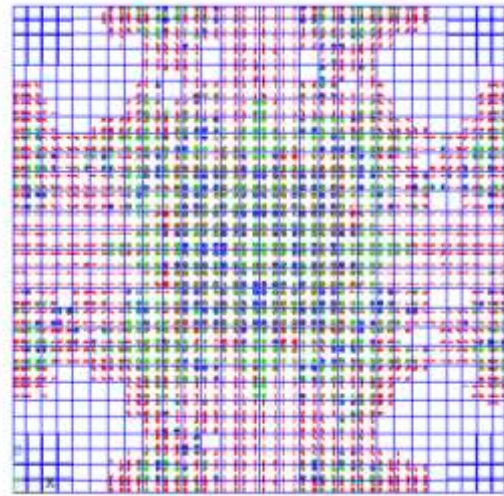
Table 8 shows the numerical and experimental ultimate loads of reinforced concrete thick slabs. The final loads for the finite element models are the last applied load steps before the solution starts to diverge due to numerous cracks and large deflections. As shown in Table 8, the numerical ultimate loads and experimental results are in a good agreement.

5.2 Crack Patterns

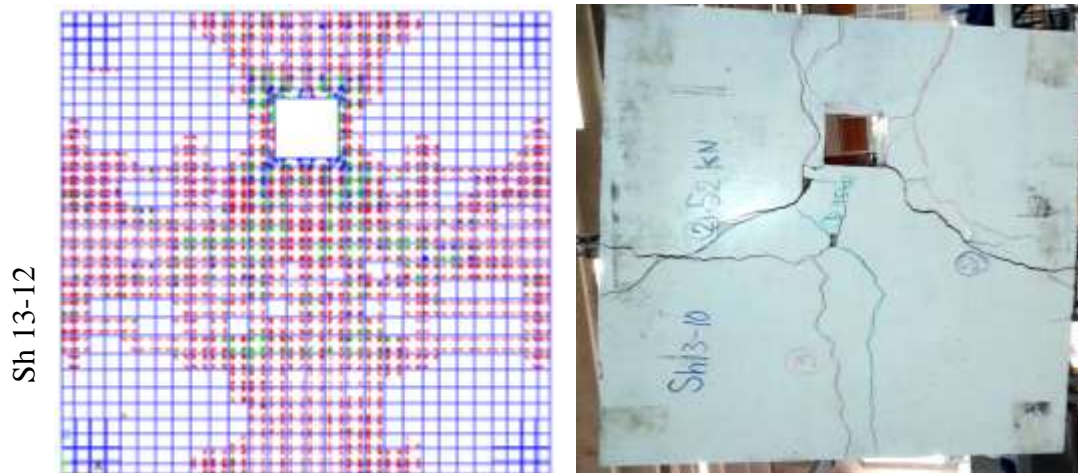
The crack patterns resulted in the finite element analysis and the failure modes of the experimental slabs agree well, as shown in Figure (10 to 12). The appearance of cracks reproduces the failure mode for the thick slab tested. The finite element model accurately predicts that the cracks are propagated in the flexural regions which formed approximately cross shape .

Table 8: Comparison Between Experimental and Finite Element Ultimate Loads

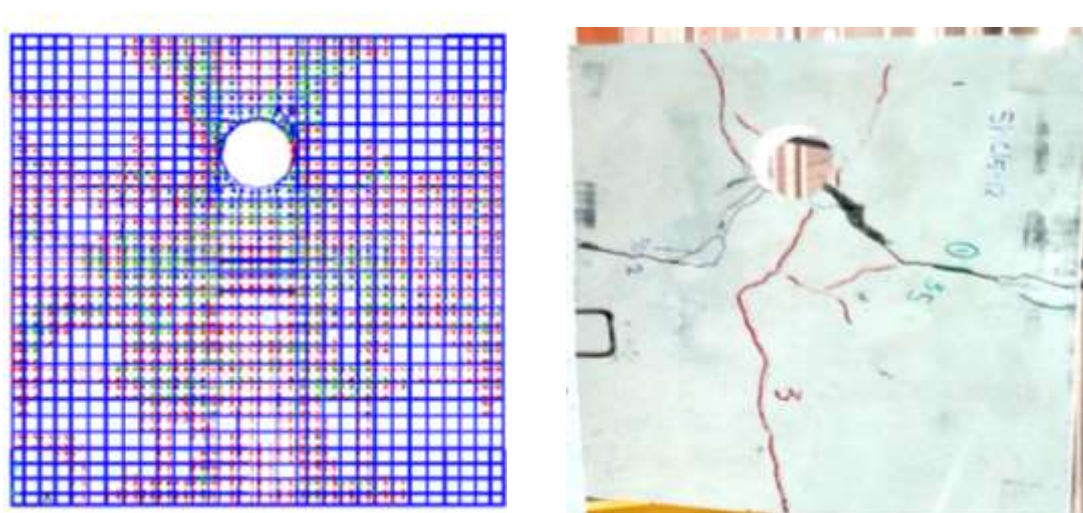
Slab Designation	Ultimate Load (kN)		$\frac{(P_u)_{EXP}}{(P_u)_{FEM}}$
	$(P_u)_{Exp.}$	$(P_u)_{F.E.M.}$	
SS 12	74.29	76.32	0.974
SS 10	60.03	61.56	0.975
SS 8	42.26	42.92	0.984
Sh13-12	63.50	62.80	1.011
Sh13-10	49.83	53.69	0.928
Sh13-8	37.13	37.75	0.984
Shc15-12	62.26	62.65	0.994
Shc15-10	46.50	45.29	1.027
Shc15-8	34.93	31.36	1.114



Figure(10): Numerical and Experimental Cracking Patterns of Thick Slab SS10 (Bottom Face).



Figure(11): Numerical and Experimental Cracking Patterns of Thick Slab Sh13-12 (Bottom Face)



Figure(12): Numerical and Experimental Cracking Patterns of Thick Slab Shc15-12 (Bottom Face)

6. CONCLUSION

- 1- Increasing the slab depth by (25 and 50)% leads to increase cracking and ultimate loads with percentage of (75 and 125)% and (42 and 75)%, respectively. Also the ratio of first cracking load to ultimate load increased according to slab depth, this ratio is (59%, 57% and 46%) for slab depth of (120, 100 and 80) mm, respectively.
- 2- The trend of deflection curves for all slabs was characterized by noticeable nonlinear behavior. Such a trend may be idealized by tri-linear diagram bounded by cracking point, yielding steel point and failure point.
- 3- For thick slabs with square openings of (130*130) mm, which have an opening dimension with span length significance of ($L/6.77$), the ultimate load reduces by (14, 17, and 12)% from solid specimens with thicknesses of (120, 100, 80) mm, respectively.
- 4- For thick slabs with circular openings of (150) mm in diameter, which have an opening dimension with span length significance of ($L/5.87$), the ultimate load reduces at about (16, 23, and 17)% from solid specimens with thicknesses of (120, 100, and 80) mm respectively.
- 5- Thick slabs with circular opening have smaller ultimate loads compared with slabs of square opening, which have an equivalent areas of openings, the ultimate load of slabs with circular opening reduces by (2, 7 and 6)% from slabs of equivalent square openings with thicknesses of (120, 100, and 80) mm, respectively.
- 6- When the slab opening is changed from square to circular shape an increase in deflection of (20%) is approximately obtained at the same load level.
- 7- The crack patterns obtained for modeled thick slabs using the finite element models are similar to the crack patterns observed in the experimental work.
- 8- The load deflection curves for thick slabs from FEA results have a good agreement with the experimental curves in the initial loading up to the yielding load.
- 9- The three-dimensional finite element model used in the present work proved its ability to simulate the behavior of RC thick slabs under static loading. Comparisons of the FEM results with the experimental data show that average difference in ultimate load for the tested slabs was 1.2%.
- 10- Although, the ultimate loads had been accurately predicted, large displacements with hardening behavior when the specimens were severely cracked had not been predicted in presented ANSYS model due to numerical problems when large regions of structure are fully plasticized.

REFERENCES

- [1] Wang, C. M., Lim, G. T., Reddy, J. N, Lee, K. H., "Relationships Between Bending Solutions of Reissner and Mindlin Plate Theories", Engineering Structures, vol. 23, 2001, pp. 838-849.
- [2] Taljsten B., Lundqvist J., Enochsson O., Rusinowski P. and Olofsson T. "CFRP Strengthened Openings in Two-way Concrete Slabs – An Experimental and Numerical Study", Construction and Building Materials, 2006, pp.810-826.
- [3] ASTM C 39/C 39M-05, "Standard Test Method for Compressive Strength of Cylindrical Concrete Specimens", Manual Book of ASTM Standards, Vol. 04.02 Concrete and Aggregates, West Conshohocken, PA, United States, 2005, 7 p.
- [4] ASTM C 496/C 496M-04, "Standard Test Method for Splitting Tensile Strength of Cylindrical Concrete Specimens", Manual Book of ASTM Standards, Vol. 04.02 Concrete and Aggregates, West Conshohocken, PA, United States, 2004, pp.5.
- [5] ASTM C 78-02, "Standard Test Method for Flexural Strength of Concrete" Manual Book of ASTM Standards, Vol. 04.02 Concrete and Aggregates, West Conshohocken, PA, United States, 2002, 3 p.
- [6] ASTM C 469-02, "Standard Test Method for Static Modulus of Elasticity and Poisson's Ratio of Concrete in Compression", Manual Book of ASTM Standards, Vol. 04.02 Concrete and Aggregates, West Conshohocken, PA, United States, 2002, 5 p.
- [7] ASTM A615/615M-05a, "Standard Specification for Deformed and Plain Carbon Structural Steel Bars for Concrete Reinforcement", Manual Book of ASTM Standards, Vol.01.02, 2005. 5p.
- [8] ANSYS, "ANSYS Help", Release 11.0, Copyright 2007.